

# Stabilization of sulfenyl(poly)selenide ions in *N,N*-dimethylacetamide

Abdelkader Ahrika, Julie Robert, Meriem Anouti and Jacky Paris\*

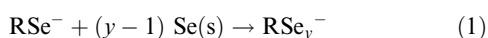
Laboratoire de Physicochimie des Interfaces et des Milieux Réactionnels, UFR Sciences et Techniques, Parc de Grandmont, 37200, Tours, France. E-mail: paris@univ-tours.fr

Received (in Montpellier, France) 16th January 2002, Accepted 27th May 2002

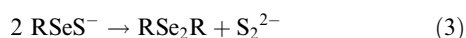
First published as an Advance Article on the web 5th September 2002

Whereas redox processes resulted from the reactions  $\text{PhSe}^-/\text{S}_8$  or  $\text{PhSe}_2\text{Ph}/\text{S}_3^{*-}$ , mixed anions  $\text{RSSe}_y^-$  ( $\text{R} = \text{Ph}, \text{PhCH}_2$ ;  $y = 1-3$ ) were obtained by the slow addition of solid selenium to thiolate ions in *N,N*-dimethylacetamide. The  $\text{RS}^- + n \text{Se}$  reactions, which were investigated by spectroelectrochemistry, led initially ( $n = 1$ ) only to the formation of  $\text{RSSe}^-$  ions. These species oxidized into  $\text{RS}_2\text{R}$  faster than  $\text{RS}^-$  on a gold electrode, with the simultaneous electrodeposition of very reactive microcrystals of selenium. On a preparative scale, the substitution of  $\text{RSSe}^-$  ions ( $\text{R} = \text{CH}_3, \text{Ph}$ ) on alkyl halides yielded  $\text{RSSeR}'$  compounds ( $\text{R}' = \text{PhCH}_2, \text{CH}_3$ , respectively) which greatly disproportionated. Further additions of  $\text{Se}$  ( $n = 2, 3$ ) to  $\text{RS}^-$  ions led to  $\text{RSSe}_2^-$  and  $\text{RSSe}_3^-$  in equilibrium with  $\text{RS}_2\text{R}$  and mixtures of  $\text{Se}_x^{2-}$  polyselenide ions ( $x = 4, 6, 8$ ). Visible spectra of  $\text{RSSe}_2^-$  and  $\text{RSSe}_3^-$  ions were calculated from the study of the backward reactions  $\text{RS}_2\text{R} + \text{Se}_x^{2-}$  ( $x = 4, 6$ ).

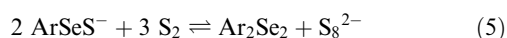
We previously reported that solid selenium slowly reacts with  $\text{RSe}^-$  selenolate ions in *N,N*-dimethylacetamide (DMA), a dipolar aprotic medium, yielding successively  $\text{RSe}_y^-$  ions [eqn. (1);  $\text{R} = \text{Ph}, \text{PhCH}_2$ ;  $y = 2-4$ ].<sup>1</sup>  $\text{RSe}_3^-$  and  $\text{RSe}_4^-$  ions disproportionate [eqn. (2)] into diselenes and  $\text{Se}_x^{2-}$  polyselenide ions which had been characterized ( $x = 4, 6, 8$ ).<sup>2</sup>



Reactions (1) are similar to those observed between sulfur and thiolates leading to  $\text{RS}_y^-$  ions ( $\text{R} = \text{alkyl}$ ,  $y = 2-5$ ).<sup>3</sup> However, very little is known about 'mixed anions' such as  $\text{RSSe}_y^-$  or  $\text{RSeS}_y^-$  ( $y \geq 1$ ): a variety of selenenyl thiolates ( $\text{RSeS}^-\text{Li}^+$ ) resulting from the addition of one sulfur unit to lithium alkyl selenolates ( $\text{RSe}^-\text{Li}^+$ ) in THF were characterized *in situ* by <sup>77</sup>Se NMR at 193 K;<sup>4</sup> however 'RSeS' readily underwent internal redox-reactions below room temperature' [eqn. (3)], and  $\text{RS}^- + \text{Se}$  (or Te) processes were described as ineffective in THF.<sup>4</sup>

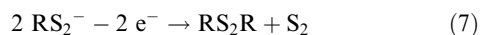
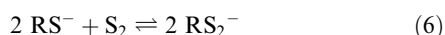


Using UV-visible absorption spectrophotometry, we recently showed that the stoichiometric addition of sulfur to selenolate ions  $2\text{-NO}_2\text{C}_6\text{H}_4\text{Se}^-$  ( $\text{ArSe}^-$ ,  $\lambda_{\text{max}} = 520 \text{ nm}$ ;  $[\text{S}]_{\text{ad}}/[\text{ArSe}^-]_0 = 1$ ) yielded  $\approx 85\%$  of  $\text{ArSeS}^-$  ions ( $\lambda_{\text{max}} = 728 \text{ nm}$ );<sup>5</sup> these species being partly oxidized in the presence of excess sulfur [eqn. (5)]:<sup>5</sup>

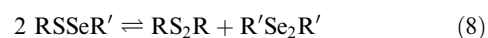


While the formation of  $\text{ArSe}_2^-$  as in eqn. (4) ( $\text{ArSe}^- + \text{Se}$ ) was complete, the conversion of  $\text{ArS}^-$  into  $\text{ArSSe}^-$  only reached 20%.<sup>5</sup>

It has now been established that  $\text{RS}_2^-$  ions oxidize into  $\text{RS}_2\text{R}$  faster than  $\text{RS}^-$  ions on a gold electrode, according to eqns. (6) and (7):<sup>3,6</sup>



Surprisingly, analogous anodic behaviours have been reported with  $\text{RSe}_2^{*-}$  and  $\text{ArSSe}^-$  species,<sup>5</sup> suggesting fast heterogeneous reactions between  $\text{RSe}^-$  or  $\text{ArS}^-$  ions and electrogenerated solid selenium. This hypothesis is reconsidered in the present paper which is mainly devoted to the expected stabilization of  $\text{RSSe}_y^-$  ( $y \geq 1$ ;  $\text{R} = \text{Ph}, \text{PhCH}_2$ ) and  $\text{PhSeS}^-$  ions. The reactions  $\text{RS}^-/\text{Se}$  and  $\text{PhSe}^-/\text{S}$ ,  $\text{RS}_2\text{R}/\text{Se}_x^{2-}$  ( $x = 4, 6, 8$ ) and  $\text{PhSe}_2\text{Ph}/\text{S}_3^{*-}$  were therefore followed by UV-visible spectrophotometry coupled with voltammetry (CV and rotating gold disc electrode). Natural selenium-containing compounds have been the subject of extensive studies because of their possible cancer chemopreventive properties.<sup>7,8</sup> 'Selenenyl sulfides'  $\text{RSSeR}'$  identified in *Allium* volatiles from speciation experiments,<sup>9</sup> are most frequently prepared by reactions between thiols ( $\text{RSH}$ ) and selenenyl halides ( $\text{R}'\text{SeX}$ ,  $\text{X} = \text{Br}, \text{Cl}$ ).<sup>10</sup> These species are also obtained by mixing the symmetrical products  $\text{RS}_2\text{R}$  and  $\text{R}'\text{Se}_2\text{R}'$  of the usual disproportionation (8):<sup>11</sup>



Our spectroelectrochemical results on the stabilization of  $\text{RSSe}^-$  ions were then applied on a preparative scale, to two typical alkylations of  $\text{RS}^-$  ( $\text{R} = \text{CH}_3, \text{Ph}$ ) + Se solutions.

## Results and discussion

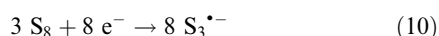
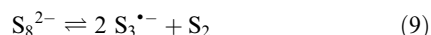
### $\text{S}_x^{2-}$ , $\text{Se}_x^{2-}$ , $\text{RS}^-$ and $\text{RSe}^-$ ions in DMA

There is now general agreement concerning the nature of polysulfide ions in dipolar aprotic media.<sup>12,13</sup> In *N,N*-dimethylacetamide, sulfur reduces in two bielectronic steps with respect to  $\text{S}_8$  on a gold rotating electrode [waves  $\text{R}_1$  and  $\text{R}_2$ ,  $E_{1/2}(\text{R}_1) = -0.40 \text{ V}$  vs. reference,  $E_{1/2}(\text{R}_2) = -1.10 \text{ V}$ ].<sup>13</sup> The electrolysis at controlled potential on the plateau of  $\text{R}_1$  occurs via the disproportionation (9) of red  $\text{S}_8^{2-}$  ions ( $\lambda_{\text{max}1} = 515 \text{ nm}$ ,  $\epsilon_{515}^8 = 3800 \text{ dm}^3 \text{ mol}^{-1} \text{ cm}^{-1}$ ;  $\lambda_{\text{max}2} = 360 \text{ nm}$ ,  $\epsilon_{360}^8 = 9000 \text{ dm}^3 \text{ mol}^{-1} \text{ cm}^{-1}$ ), up to the stable blue  $\text{S}_3^{*-}$  radical-anion ( $\lambda_{\text{max}} = 617 \text{ nm}$ ,  $\epsilon_{617}^3 = 4100 \text{ dm}^3 \text{ mol}^{-1} \text{ cm}^{-1}$ ) in equilibrium with its dimer  $\text{S}_6^{2-}$  in a minor proportion. In our opinion cyclooctasulfur is in equilibrium with the reactive  $\text{S}_2$  molecules, thus appearing in equations such as (9).<sup>13</sup>

**Table 1** Redox processes occurring at a Se-coated gold disc electrode in DMA and related peak potentials *vs.* reference Ag/AgCl, KCl sat. in DMA–NET<sub>4</sub>ClO<sub>4</sub> (0.1 mol dm<sup>−3</sup>) from CV at a scan rate of 100 mV s<sup>−1</sup>

Redox process	Peaks <sup>a</sup> (potential/V)
8Se <sub>(s)</sub> + 2e <sup>−</sup> ⇌ Se <sub>8</sub> <sup>2−</sup>	R <sub>1</sub> (−0.49) O <sub>1</sub> ' (−0.33)
3Se <sub>8</sub> <sup>2−</sup> + 2e <sup>−</sup> ⇌ 4Se <sub>6</sub> <sup>2−</sup>	R <sub>2</sub> (−0.62) O <sub>1</sub> ' (−0.33)
2Se <sub>6</sub> <sup>2−</sup> + 2e <sup>−</sup> ⇌ 3Se <sub>4</sub> <sup>2−</sup>	R <sub>3</sub> (−0.89) O <sub>2</sub> ' (−0.65)
3Se <sub>4</sub> <sup>2−</sup> + 2e <sup>−</sup> ⇌ 4Se <sub>3</sub> <sup>2−</sup> (?)	R <sub>4</sub> (−1.28) O <sub>3</sub> ' (−1.0)
2Se <sub>3</sub> <sup>2−</sup> + 2e <sup>−</sup> → 3Se <sub>2</sub> <sup>2−</sup> (?)	R <sub>5</sub> (−1.55)

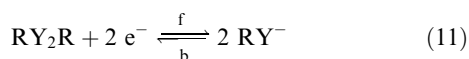
<sup>a</sup> R = cathodic; O = anodic.



S<sub>8</sub><sup>2−</sup> and S<sup>−1/3</sup> ions (S<sub>3</sub><sup>•−</sup> ⇌ S<sub>6</sub><sup>2−</sup>) oxidize (O<sub>1</sub>) and reduce (R<sub>2</sub>) at the same potentials [*E*<sub>1/2</sub>(O<sub>1</sub>) = −0.20 V; *E*<sub>1/2</sub>(R<sub>2</sub>) = −1.10 V].

Prior to this study, Se<sub>*x*</sub><sup>2−</sup> ions (*x* = 8, 6, 4) were successively obtained by coulometric reduction (R<sub>1</sub>–R<sub>3</sub> steps) of weighed amounts of grey selenium coating a large gold grid electrode.<sup>2</sup> Two further reduction steps detected on cyclic voltammograms (R<sub>4</sub>, R<sub>5</sub>, perhaps leading to Se<sub>3</sub><sup>2−</sup> and Se<sub>2</sub><sup>2−</sup> as in liquid ammonia)<sup>14</sup> were not identifiable by our method because of passivation phenomena on the gold electrode surface. The redox processes summarized in Table 1 and the known UV-visible spectra<sup>2</sup> providing molar absorbance of the stable Se<sub>*x*</sub><sup>2−</sup> ions (Fig. 1; *x* = 8, λ<sub>max</sub> = 648, 453, 398 nm; *x* = 6, λ<sub>max</sub> = 598, 440 nm; *x* = 4, λ<sub>max</sub> = 550, 417 nm) were used for quantitative data processing in this study.

RY<sup>−</sup> ions (Y = Se, R = Ph; Y = S, R = Ph, PhCH<sub>2</sub>) were generated ([RY<sup>−</sup>]<sub>0</sub> ≤ 4 × 10<sup>−3</sup> mol dm<sup>−3</sup>) by electrolysis of RY<sub>2</sub>R species at a controlled potential of a gold electrode on the plateau of their bielectronic waves (Y = Se,<sup>1,15</sup> Y = S<sup>3,16</sup>) according to previously described procedures [eqn. 11f]:



The electrochemical and spectrophotometric characteristics of RY<sub>2</sub>R and RY<sup>−</sup> species are summarized in Table 2.

#### PhSe<sub>2</sub>Ph/S<sub>3</sub><sup>•−</sup> and PhSe<sup>−</sup>/S<sub>8</sub> reactions

The addition of PhSe<sub>2</sub>Ph to S<sub>3</sub><sup>•−</sup> ions resulted in instantaneous changes in voltammograms and spectra (Fig. 2) which agreed with equilibrium (12):

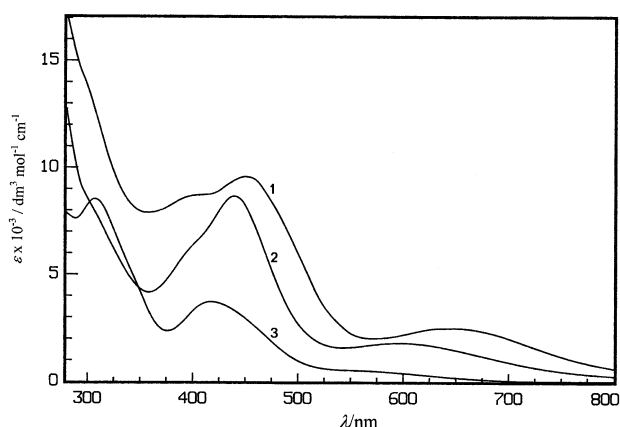


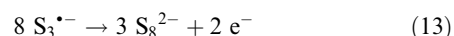
**Fig. 1** UV-visible absorption spectra ( $\epsilon_i/\text{dm}^3 \text{mol}^{-1} \text{cm}^{-1}$ ) of Se<sub>8</sub><sup>2−</sup> (1), Se<sub>6</sub><sup>2−</sup> (2) and Se<sub>4</sub><sup>2−</sup> (3) ions in dimethylacetamide.

**Table 2** Electrochemical and spectrophotometric characteristics of RY<sub>2</sub>R and RY<sup>−</sup> species (Y = Se, S) in DMA—*E*<sub>1/2</sub> at a rotating gold disc electrode *vs.* reference

R, Y	RY <sub>2</sub> R <i>E</i> <sub>1/2</sub> (R)/V	RY <sup>−</sup>		
		<i>E</i> <sub>1/2</sub> (O)/V	λ <sub>max</sub> /nm	ε <sub>max</sub> <sup>a</sup>
Ph, Se	−0.76	−0.36	318	12 700
Ph, S	−1.25	+0.02	309	18 200
PhCH <sub>2</sub> , S	−1.55	−0.03	285 <sup>b</sup>	3850

<sup>a</sup> ε<sub>i</sub>/dm<sup>3</sup> mol<sup>−1</sup> cm<sup>−1</sup>. <sup>b</sup> Shoulder.

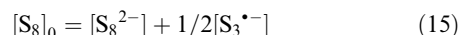
*A*<sub>617</sub>(S<sub>3</sub><sup>•−</sup>) decreased in favor of *A*<sub>515</sub> (S<sub>8</sub><sup>2−</sup> and *A*<sub>360</sub> (S<sub>8</sub><sup>2−</sup> and PhSe<sup>−</sup> in part) according to calculated Δ[S<sub>3</sub><sup>•−</sup>]/Δ[S<sub>8</sub><sup>2−</sup>] values close to −2.6 ≈ −8/3, and through the same isosbestic point (λ<sub>is</sub> = 545 nm) as in the course of electrooxidation (13) of S<sup>−1/3</sup> ions:<sup>13</sup>



However, as shown by the growth of the reduction wave of PhSe<sub>2</sub>Ph [*E*<sub>1/2</sub>(R) = −0.76 V] from the first additions of diphenyl diselenide, preceding the constant cathodic current of S<sub>3</sub><sup>•−</sup>/S<sub>8</sub><sup>2−</sup> ions [*E*<sub>1/2</sub>(R) = −1.10 V] reaction (12) was not quantitative. At the stoichiometric value [PhSe<sub>2</sub>Ph]<sub>ad</sub>/[S<sub>3</sub><sup>•−</sup>]<sub>0</sub> = 1/8 in the experimental conditions of Fig. 2, consumption of S<sup>−1/3</sup> ions only reached 40%. S<sub>8</sub><sup>2−</sup> ions remained unreactive towards PhSe<sub>2</sub>Ph since *A*<sub>515</sub> always increased with addition of the substrate in excess. Conversely, sulfur quantitatively reacted with benzene selenolate ions in accordance with eqn. (14):



With the addition of sulfur to PhSe<sup>−</sup> ions the spectra were the same as those observed when S<sub>8</sub> was electrolyzed at 2 F mol<sup>−1</sup> S<sub>8</sub> for various [S<sub>8</sub>]<sub>0</sub> concentrations,<sup>13</sup> regardless of [S]<sub>ad</sub>/[PhSe<sup>−</sup>]<sub>0</sub> ratio values between 0 and 1: the increases of absorbances at 515 nm (S<sub>8</sub><sup>2−</sup>) and 617 nm (S<sub>3</sub><sup>•−</sup>) because of the partial disproportionation (9) with a negligible sulfur proportion always confirmed (±6%) the conservation eqn. (15):



At the same time, the reduction currents of PhSe<sub>2</sub>Ph [*E*<sub>1/2</sub>(R) = −0.76 V] and of S<sub>3</sub><sup>•−</sup>/S<sub>8</sub><sup>2−</sup> ions [*E*<sub>1/2</sub>(R) = −1.10 V] increased, while the anodic wave of the latter [*E*<sub>1/2</sub>(O) = −0.20 V] progressively replaced that of PhSe<sup>−</sup> ions [*E*<sub>1/2</sub>(O) = −0.36 V] up to stoichiometry (14).

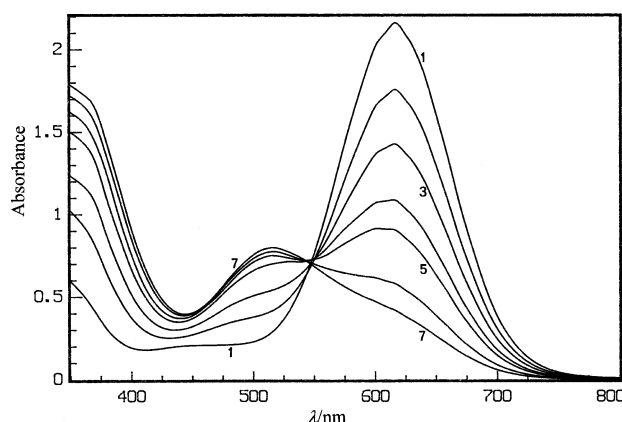


**Fig. 2** Dependence of the UV-visible spectra on the addition of diphenyl diselenide to a [S<sub>3</sub><sup>•−</sup>]<sub>0</sub> = 6.06 × 10<sup>−3</sup> mol dm<sup>−3</sup> solution. [PhSe<sub>2</sub>Ph]<sub>ad</sub>/[S<sub>3</sub><sup>•−</sup>]<sub>0</sub> = 0 (1); 0.063 (2); 0.125 (3); 0.23 (4); 0.32 (5); 0.503 (6); 0.96 (7). Thickness of the cell = 0.1 cm; scan rate = 500 nm min<sup>−1</sup>.

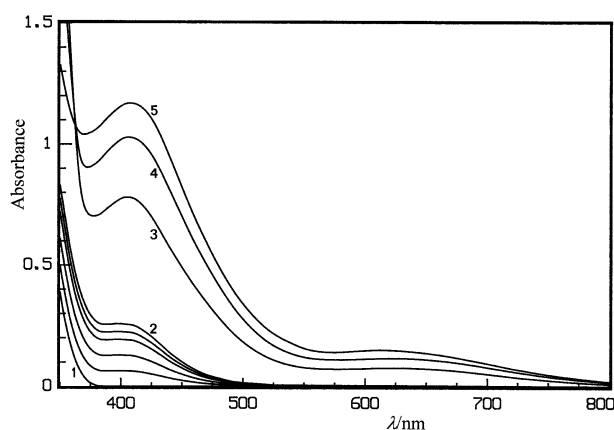
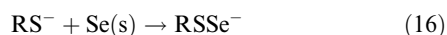


**Fig. 3** Changes in UV-visible spectra with the addition of selenium powder to a  $[\text{PhS}^-]_0 = 2.87 \times 10^{-3} \text{ mol dm}^{-3}$  solution.  $n = (\text{Se})_{\text{ad}}/(\text{RS}^-)_0 = 0$  (1); 0.99 (2); 1.98 (3); 2.99 (4); 4.0 (5); recordings at equilibrium except for (1)  $\rightarrow$  (2),  $A = f(t)$ ,  $0 < t < 95 \text{ min}$ .

Thus, in contrast to the two successive steps which were evidenced in the course of the addition of sulfur to the least reducing  $2\text{-NO}_2\text{C}_6\text{H}_4\text{Se}^-$  ( $\text{ArSe}^-$ ) species,<sup>5</sup> formation (4) of  $\text{ArSeS}^-$ , then reversible oxidation (5) into  $\text{ArSe}_2\text{Ar}$ , only redox processes (12) and (14) resulted from the reactions  $\text{PhSe}_2\text{Ph}/\text{S}_3^{2-}$  and  $\text{PhSe}^-/\text{S}_8$ , respectively, without any observed stabilization of  $\text{PhSeS}^-$  ions.

#### Stabilization and electrocatalytic oxidation of $\text{RSSe}^-$ ions

When grey selenium powder (pellets, diameter *ca.* 10–30  $\mu\text{m}$ ) was added to stirred solutions of  $\text{PhS}^-$  and  $\text{PhCH}_2\text{S}^-$  ions at a ratio  $n = (\text{Se})_{\text{ad}}/(\text{RS}^-)_0 = 1$ , the changes in UV-visible spectra and cyclic voltammograms were similar in both cases, as illustrated in Figs. 3 and 4 ( $\text{R} = \text{Ph}$ ). In the course of the Se consumption which required about 1.5 h up to  $n = 1$ , two absorption bands regularly increased with time:  $\text{R} = \text{Ph}$  (see Fig. 3, curves 1  $\rightarrow$  2),  $\lambda_{\text{max}1} = 403 \text{ nm}$ ,  $\lambda_{\text{max}2} = 260 \text{ nm}$ , isosbestic point  $\lambda_{\text{is}} = 272 \text{ nm}$ ;  $\text{R} = \text{PhCH}_2$ ,  $\lambda_{\text{max}1} = 430 \text{ nm}$ ,  $\lambda_{\text{max}2} = 260 \text{ nm}$ ,  $\lambda_{\text{is}1} = 324 \text{ nm}$ ,  $\lambda_{\text{is}2} = 298 \text{ nm}$ ), in agreement with the formation of only  $\text{RSSe}^-$  ions:



As soon as solid Se was added, and before any growth of absorbance at about 400 nm, the oxidation current of  $\text{RS}^-$

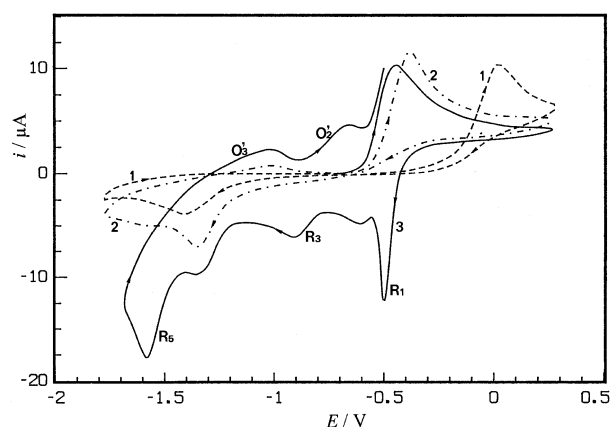


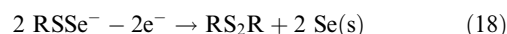
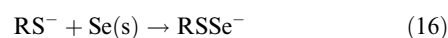
**Fig. 4** Cyclic voltammograms of a  $[\text{PhS}^-]_0 = 3.52 \times 10^{-3} \text{ mol dm}^{-3}$  (0.14 mmol) solution (1) added with selenium powder (11 mg, 0.14 mmol);  $\Delta t = 2 \text{ min}$  (2); 92 min (3).  $E$  vs.  $\text{Ag}/\text{AgCl}$ ,  $\text{KCl}$  sat. in  $\text{DMA-NEt}_4\text{ClO}_4$  0.1  $\text{mol dm}^{-3}$ . Scan rate = 50  $\text{mV s}^{-1}$ .

**Table 3**  $\Delta E_{1/2}(\text{O})/\text{V}$  variation of anodic half-wave potentials<sup>a</sup> related to the oxidations of  $\text{RYZ}^-$  and  $\text{RY}^-$  ions into  $\text{RY}_2\text{R}$  species

	$\text{R} = \text{Ph}$	$\text{R} = \text{PhCH}_2$	$\text{R} = \text{Ar}^b$
$\text{Y, Z} = \text{S, S}$	−0.23	−0.46	−0.50
$\text{Y, Z} = \text{Se, Se}$	−0.08	−0.06	−0.41
$\text{Y, Z} = \text{S, Se}$	−0.47	−0.35	−0.68

<sup>a</sup>  $\Delta E_{1/2}(\text{O}) = E_{1/2}(\text{RYZ}^-) - E_{1/2}(\text{RY}^-)$ . <sup>b</sup>  $\text{Ar} = 2\text{-NO}_2\text{C}_6\text{H}_4$ .

ions into  $\text{RS}_2\text{R}$  [Fig. 4, curve 1,  $E_p^a = +0.04 \text{ V}$ ,  $E_p^c = -1.40$ – $-1.40 \text{ V}$ ] totally shifted towards less anodic potentials (curve 2,  $E_p^a = -0.37 \text{ V}$ ). At the end of reaction (16)  $\text{PhSSe}^-$  had an oxidation peak at  $-0.44 \text{ V}$  (curve 3), and reversal of the voltage scan direction resulted in the appearance of the sharp reduction peak of electrodeposited Se [ $E_p^c(1) = -0.49 \text{ V}$ ]<sup>2</sup> followed by the subsequent cathodic peaks 2–5 of the polyselenide ions (Table 1), then associated anodic peaks (3', 2'). This electrochemical behavior of  $\text{RS}^-$  ions in the presence of selenium complies with the following electrocatalytic mechanism [eqns. (16)–(18)], which is analogous to those previously reported for  $\text{RS}^-/\text{RS}_2^{3,6}$  and  $\text{RSe}^-/\text{RSe}_2^-$  species:<sup>1</sup>



Thus,  $\text{RS}_2^-$ ,  $\text{RSe}_2^-$  and  $\text{RSSe}^-$  ions oxidize into  $\text{RY}_2\text{R}$  ( $\text{Y} = \text{S, Se}$ ) on a gold electrode, at a greater rate than  $\text{RY}^-$  ions, as shown by the differences between their respective half-wave potentials of oxidation listed in Table 3. The occurrence of the catalytic processes from the addition of insoluble selenium to  $\text{RY}^-$  ions ( $\text{Y} = \text{S, Se}$ ) implies fast heterogeneous reactions such as in eqn. (16) between  $\text{RY}^-$  and the released Se in the course of electrooxidation [*e.g.*, eqn. (18)], although  $\text{RSe}_2^-$  or  $\text{RSSe}^-$  were only obtained by direct addition (1) or (16) after 1.5 hour. The same schemes were tested on quantitative electrolysis at a controlled potential of a large gold grid electrode ( $E = -0.10 \text{ V}$ ), of a solution containing  $\text{ArSe}^-$  [ $\text{Ar} = 2\text{-NO}_2\text{Ph}$ ,  $E_{1/2}(\text{O}) = +0.16 \text{ V}$ ,  $\lambda_{\text{max}} = 520 \text{ nm}$ ,  $\epsilon_{\text{max}} = 1200 \text{ dm}^3 \text{ mol}^{-1} \text{ cm}^{-1}$ ]<sup>5</sup> and  $\text{ArSe}_2^-$  [ $E_{1/2}(\text{O}) = -0.25 \text{ V}$ ,  $\lambda_{\text{max}} = 728 \text{ nm}$ ,  $\epsilon_{\text{max}} = 3450 \text{ dm}^3 \text{ mol}^{-1} \text{ cm}^{-1}$ ]<sup>5</sup> ions:  $[\text{ArSe}^-]_0 = 3.40 \times 10^{-3} \text{ mol dm}^{-3}$ ,  $[\text{ArSe}_2^-]_0 = 2.25 \times 10^{-3} \text{ mol dm}^{-3}$  [spectral changes in Fig. 5 as a function of  $z \text{ F mol}^{-1}$  ( $\text{ArSe}^-)_0 + (\text{ArSe}_2^-)_0$ ]. As long as  $\text{ArSe}^-$  ions were in greater

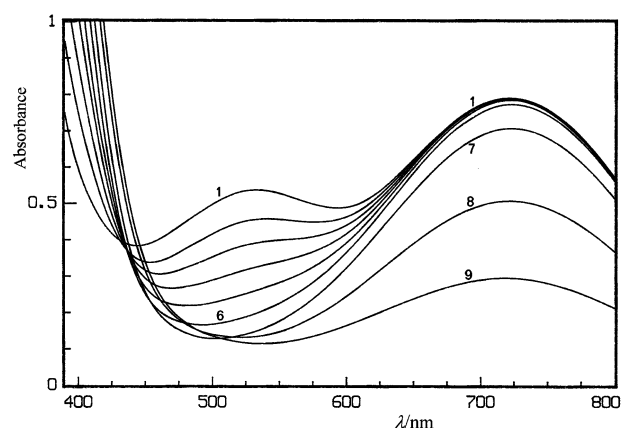
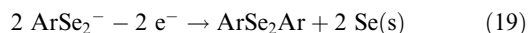


**Fig. 5** Spectral changes in the course of the electrooxidation at  $E = -0.10 \text{ V}$  vs. reference of a  $[\text{ArSe}^-]_0 = 3.40 \times 10^{-3} \text{ mol dm}^{-3}$  +  $[\text{ArSe}_2^-]_0 = 2.25 \times 10^{-3} \text{ mol dm}^{-3}$  solution ( $\text{Ar} = 2\text{-NO}_2\text{Ph}$ ):  $z \text{ F mol}^{-1}$  ( $\text{ArSe}^-)_0 + (\text{ArSe}_2^-)_0 = 0$  (1)–0.58 (6); 0.65 (7); 0.75 (8); 0.85 (9).

concentration than initially added Se ( $[\text{ArSe}^-] > [\text{ArSe}_2^-]_0$ ,  $z < 0.60$ , curves 1–6), the decrease in  $A_{520}$  was in accordance with the oxidation of  $\text{ArSe}^-$  ions into  $\text{ArSe}_2\text{Ar}$  (growth of its cathodic wave,  $E_{1/2} = -0.69 \text{ V}$ )<sup>5</sup> at a potential ( $E = -0.10 \text{ V}$ ) only suited to that of  $\text{ArSe}_2^-$  [eqn. (19)]:



Simultaneously  $A_{728}$  ( $\text{ArSe}_2^-$ ) remained at a constant value because of the ‘instantaneous’ reaction between  $\text{ArSe}^-$  and Se which was generated at the electrode surface. Then ( $z > 0.60$ ), curves 7–9), the consumption of  $\text{ArSe}_2^-$  (decrease in  $A_{728}$ ) resulted in the deposition of solid selenium on the gold grid, and the recovery of  $\text{ArSe}_2\text{Ar}$  ( $z \approx 1.05$ ) according to its characteristic absorption at 378 nm ( $\epsilon_{\text{max}} = 7300 \text{ dm}^3 \text{ mol}^{-1} \text{ cm}^{-1}$ ).<sup>5</sup>

Similarly, a gold foil ( $1 \times 1 \text{ cm}$ ) was coated with grey selenium by electrolysis ( $E = -0.25 \text{ V}$ ) of  $\text{PhSSe}^-$  ions (about 0.076 mmol), and then observed by scanning electron microscopy (SEM). The SEM images shown in Figs. 6a–6b revealed an epicentric crystallization with small dendrites, mostly 1 to 2  $\mu\text{m}$  in length, which could explain the high reactivity of ‘Se-nucleophiles’ such as  $\text{RY}^-$  species ( $Y = \text{S, Se}$ ) towards electrogenerated selenium.

The recent interest in biochemistry of  $\text{RSSeR}'$  species<sup>7–9</sup> led us to examine the alkylation of two  $\text{RSSe}^-$  solutions on a preparative scale as examples:  $\text{CH}_3\text{SSe}^- + \text{PhCH}_2\text{Br}$  and  $\text{PhSSe}^- + \text{CH}_3\text{I}$ . The compositions of the mixtures of products  $\text{RSSeR}'$ ,  $\text{RS}_2\text{R}$ ,  $\text{R}'\text{Se}_2\text{R}'$  which were analyzed by  $^1\text{H}$  NMR and GC/MS (see Experimental) corresponded to significant disproportionation of the expected selenenyl sulfides  $\text{CH}_3\text{SSeCH}_2\text{Ph}$  ( $\approx 80\%$ ) and  $\text{PhSSeCH}_3$  ( $\approx 70\%$ ), as previously reported for this class of rather unstable compounds [eqn. (8)].<sup>11</sup>

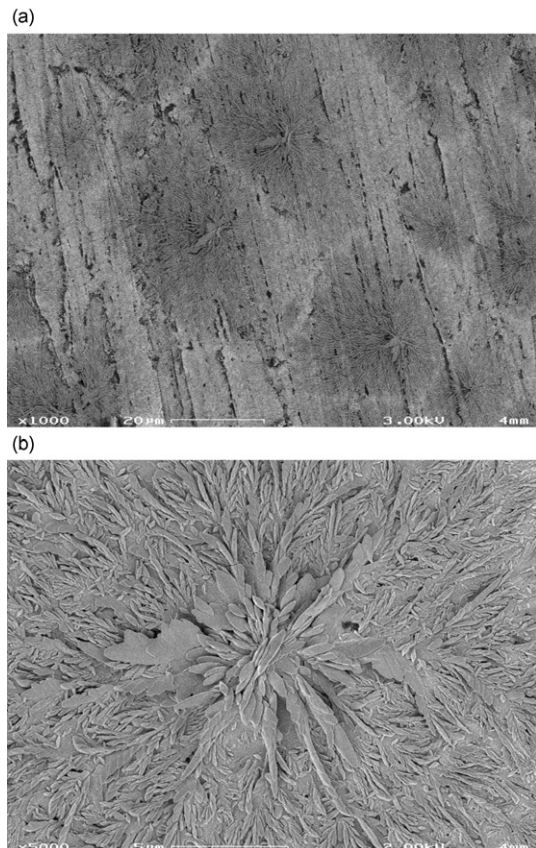


**Fig. 6** Scanning electron micrographs of electrodeposited selenium on a gold foil from the oxidation of  $\text{PhSSe}^-$  ions ( $E = -0.25 \text{ V}$ ). (a)  $\times 1000$ ; (b)  $\times 5000$ .

## Formation of $\text{RSSe}_y^-$ ions

Further additions of solid selenium to  $\text{RSSe}^-$  ions [ $\text{R} = \text{Ph, PhCH}_2$ ,  $n = (\text{Se})_{\text{ad}}/(\text{RSSe}^-)_0$  greater than 1] resulted in its total consumption within 2 h ( $n = 2$ ), then 2.5 h ( $n = 3$ ), whereas traces of solid Se remained unreactive for  $n = 4$  beyond 4 h. The partial oxidation of the anionic solutions was shown by the appearance of  $\text{Se}_x^{2-}$  ions ( $x \geq 4$ ). Mixtures of these species were detected by the simultaneous increase in their absorption at around 625 nm ( $\text{Se}_6^{2-}/\text{Se}_8^{2-}$ ,  $\text{R} = \text{Ph}$ , Fig. 3, curves 3–5) or 590–620 nm ( $\text{Se}_4^{2-}/\text{Se}_6^{2-}$  or  $\text{Se}_6^{2-}/\text{Se}_8^{2-}$ ,  $\text{R} = \text{PhCH}_2$ ), and in their reduction waves (RDE,  $x = 8, 6, 4$ ;  $E_{1/2} = -0.55, -0.83, -1.20 \text{ V}$ ),<sup>2</sup> with greater currents at potentials close to those of  $\text{RS}_2\text{R}$  ( $\text{R} = \text{Ph}$ ,  $E_{1/2} \approx -1.25 \text{ V}$ ;  $\text{R} = \text{PhCH}_2$ ,  $E_{1/2} \approx -1.55 \text{ V}$ ). At the same time another absorption band increased at about 405 nm ( $\text{R} = \text{Ph}$ ) or 380 nm ( $\text{R} = \text{PhCH}_2$ ) which could not be related to  $\text{Se}_x^{2-}$  ions from the shape of their own spectra (Fig. 1). Moreover, spectra and voltammograms were the same when equilibrium was attained for the respective stoichiometries:  $\text{RS}^- + 2 \text{Se}$  ( $\text{R} = \text{Ph}$ , Fig. 3, curve 3) and  $\text{RS}_2\text{R} + \text{Se}_4^{2-}$ ;  $\text{RS}^- + 3 \text{Se}$  (Fig. 3, curve 4) and  $\text{RS}_2\text{R} + \text{Se}_6^{2-}$  (see below Fig. 7, curve 5). All of these observations were analogous to those occurring in the course of the  $\text{RSe}^- + n \text{Se(s)}$  ( $n \geq 2$ ) and  $\text{RSe}_2\text{R} + \text{Se}_x^{2-}$  ( $x = 4, 6$ ) reactions, which yielded  $\text{RSSe}_y^-$  ions ( $y = 3, 4$ , maximal absorbances at 400–420 nm) in equilibrium with  $\text{RSe}_2\text{R}$  and mixtures of polyselenide ions [eqn. (2)].<sup>1</sup> Here again, the fast reactions  $\text{RS}_2\text{R} + \text{Se}_x^{2-}$  ( $\text{R} = \text{Ph, PhCH}_2$ ;  $x = 4, 6$ ) were followed by calculations first of the polyselenide concentrations as a function of  $m = [\text{RS}_2\text{R}]_{\text{ad}}/[\text{Se}_x^{2-}]_0$ :  $[\text{Se}_6^{2-}]$  and  $[\text{Se}_8^{2-}]$  ( $598 < \lambda_{\text{max}} < 648 \text{ nm}$ ), or  $[\text{Se}_4^{2-}]$  and  $[\text{Se}_6^{2-}]$  ( $550 < \lambda_{\text{max}} < 598 \text{ nm}$ ), were deduced from experimental values of  $A_{598}$  and  $A_{648}$  or  $A_{598}$  and  $A_{550}$ , respectively, by the use of the known  $\epsilon_i$  molar absorptivity (Fig. 1), e.g. eqn. (20),  $\epsilon_i$  ( $\text{dm}^3 \text{ mol}^{-1} \text{ cm}^{-1}$ ,  $\pm 4\%$ ):  $\epsilon_{598}^6 = 1750$ ,  $\epsilon_{598}^8 = 2150$ ;  $\epsilon_{648}^8 = 2500$ ,  $\epsilon_{648}^6 = 1450$ .<sup>1</sup>

$$A_i = \epsilon_i(\text{Se}_6^{2-})[\text{Se}_6^{2-}] + \epsilon_i(\text{Se}_8^{2-})[\text{Se}_8^{2-}] \quad (20)$$

The other concentrations  $[\text{RS}_2\text{R}]$  and  $[\text{RSSe}_y^-]$ , as well as the average number  $\bar{y}$  of Se units in  $\text{RSSe}_y^-$  chains, were then calculated by solving the conservation equations from  $[\text{RS}_2\text{R}]_{\text{ad}}$  and  $[\text{Se}_x^{2-}]_0$  values. As an example, Fig. 7 shows the changes in spectra for the reaction  $\text{PhS}_2\text{Ph} + \text{Se}_6^{2-}$ . Two steps can be distinguished:

(i) for  $0 < m \leq 0.42$  (curves 1–2), the maximal absorbance of  $\text{Se}_6^{2-}$  ions ( $A_{440}$ ,  $A_{598}$ ) evolved towards that of  $\text{Se}_8^{2-}$  ( $A_{398}$ ,  $A_{453}$ ,  $A_{648}$ ) through three isosbestic points ( $\lambda_{\text{is}} = 398, 474$  and  $545 \text{ nm}$ ), according to the rough stoichiometry of eqn. (21):

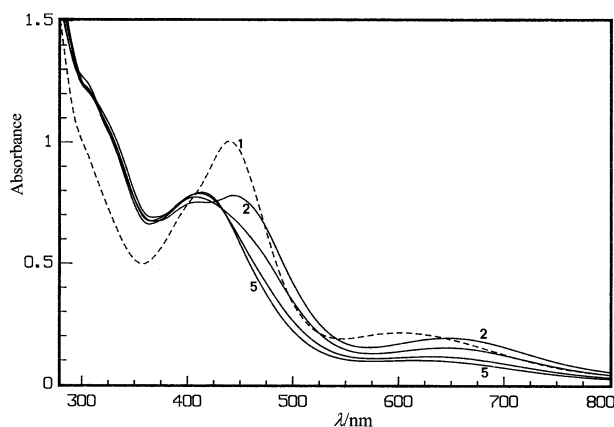
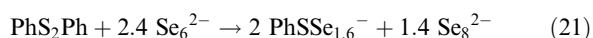


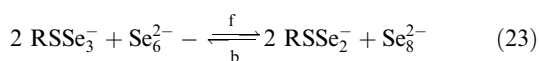
**Fig. 7** Changes in UV-visible spectra with the addition of diphenyl disulfide to a  $[\text{Se}_6^{2-}]_0 = 1.15 \times 10^{-3} \text{ mol dm}^{-3}$  solution:  $m = [\text{RS}_2\text{R}]_{\text{ad}}/[\text{Se}_6^{2-}]_0 = 0$  (1); 0.42 (2); 0.66 (3); 0.90 (4); 1.02 (5).

**Table 4** Calculated compositions of solutions at equilibrium for the reactions  $\text{RS}_2\text{R} + \text{Se}_x^{2-}$  ( $x = 4, 6$ ) and  $\text{RS}^- + n \text{Se}$  ( $n = 2, 3$ ) depending on initial conditions<sup>a</sup>

Initial cond. <sup>a</sup>	$[\text{Se}_4^{2-}]$	$[\text{Se}_6^{2-}]$	$[\text{Se}_8^{2-}]$	$[(\text{RS})_2]$	$[(\text{RSSe}_y^-)]$	$\bar{y}$
$[(\text{PhS})_2]_0 = 2.70 + [\text{Se}_4^{2-}]_0 = 2.74$	—	0.42	0.21	0.60	4.20	1.6
$[\text{PhS}^-]_0 = 2.87 + [\text{Se}]_0 = 5.70$	—	0.23	0.15	0.38	2.11	1.5
$[(\text{PhS})_2]_0 = 1.12 + [\text{Se}_6^{2-}]_0 = 1.10$	—	0.35	0.17	0.54	1.16	2.7
$[\text{PhS}^-]_0 = 2.87 + [\text{Se}]_0 = 8.58$	—	0.37	0.22	0.59	1.69	2.7
$[(\text{PhCH}_2\text{S})_2]_0 = 2.54 + [\text{Se}_4^{2-}]_0 = 2.66$	0.54	0.22	—	0.64	3.80	1.9
$[\text{PhCH}_2\text{S}^-]_0 = 2.90 + [\text{Se}]_0 = 5.70$	0.40 <sub>5</sub>	0.10 <sub>5</sub>	—	0.51	1.88	1.8 <sub>5</sub>
$[(\text{PhCH}_2\text{S})_2]_0 = 1.59 + [\text{Se}_6^{2-}]_0 = 1.54$	—	0.47 <sub>5</sub>	0.20	0.72	1.74	2.7 <sub>5</sub>
$[\text{PhCH}_2\text{S}^-]_0 = 2.90 + [\text{Se}]_0 = 8.60$	—	0.44 <sub>5</sub>	0.22 <sub>5</sub>	0.67	1.56	2.6 <sub>5</sub>

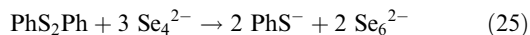
<sup>a</sup> All concentrations are in  $\text{mmol dm}^{-3}$ .

(ii) for  $0.42 < m \leq 1.0$  (curves 2–5), the progressive displacement  $A_{648} \rightarrow A_{618}$  agreed with a partial recovery of  $\text{Se}_6^{2-}$  ions, and with the formation at the same time of  $\text{RSSe}_y^-$  ions of higher  $\bar{y}$  rank (Table 4,  $m = 1$ ,  $\bar{y} = 2.7$ ), giving a maximum absorbance at about 412 nm. These results can be explained by eqns. (22)–(24):

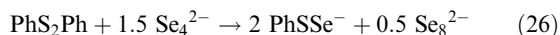


In the presence of  $\text{Se}_6^{2-}$  ions in excess ( $m < 0.42$ ), reactions (22) and (23) totally shift to the right, leading to a mixture of  $\text{RSSe}^-$  and  $\text{RSSe}_2^-$  ions by equilibrium (24) ( $\bar{y} \approx 1.6$ ). With further additions of  $\text{RS}_2\text{R}$ , the consumption of  $\text{Se}_6^{2-}$  displaces equilibria (23) and (24) in reverse, increasing the  $\bar{y}$  value to 2.7 (mixture  $\text{RSSe}_2^-/\text{RSSe}_3^-$ ).

Similarly, three steps were observed from progressive changes in  $A = f(\lambda)$  curves during the addition of  $\text{PhS}_2\text{Ph}$  to the more reducing  $\text{Se}_4^{2-}$  ions: (i)  $0 < m \leq 0.35$ ,  $A_{550} \rightarrow A_{598}$  and  $A_{417} \rightarrow A_{440}$ , and thus  $\text{Se}_4^{2-} \rightarrow \text{Se}_6^{2-}$  according to the nearly quantitative redox process (25).



(ii)  $0.35 < m \leq 0.67$ ,  $A_{598} \rightarrow A_{645}$  and  $A_{440} \rightarrow A_{450}/A_{400}$  due to further reaction of  $\text{Se}_6^{2-}$  ions which provided  $\text{Se}_8^{2-}$  ions in accordance with the overall eqn. (26).



(iii)  $0.67 < m < 1.0$ ,  $A_{645} \rightarrow A_{615}$  and  $A_{450}/A_{400} \rightarrow A_{407}$ ; the reactions of  $\text{Se}_6^{2-}/\text{Se}_8^{2-}$  ions finally led to  $\bar{y} \approx 1.6$  ( $m = 1$ ) by ‘Se-exchanges’ as in eqn. (24).

The calculated concentrations and average  $\bar{y}$  numbers at the end of slow reactions  $[\text{RS}^-]_0 + n (\text{Se})_{\text{ad}}$  ( $\text{R} = \text{Ph}, \text{PhCH}_2$ ;  $n = 2, 3$ ) and of the equivalent fast reactions  $[\text{RS}_2\text{R}]_0 + [\text{Se}_x^{2-}]_0$  ( $m = 1$ ;  $x = 4, 6$ ) are given in Table 4. Based on  $[\text{RS}_2\text{R}]$  values at equilibrium compared with  $[\text{RS}^-]_0$  or  $[\text{RS}_2\text{R}]_0$  (Table 4,  $\text{R} = \text{Ph}$  and  $\text{PhCH}_2$ ), the disproportionations of  $\text{RSSe}_y^-$  ions could therefore be roughly situated at ca. 25% ( $y = 2$ ) and 45% ( $y = 3$ ). These levels meet those of  $\text{RSe}_3^-$  (30%) and  $\text{RSe}_4^-$  (~45%) ions [eqn. (2)].<sup>1</sup> Furthermore, the spectra of  $\text{RSSe}_y^-$  ions ( $y = 2, 3$ ) were obtained over the wavelength range 350–600 nm as previously obtained for  $\text{RSe}_3^-$  and  $\text{RSe}_4^-$  ions:<sup>1</sup> (i)  $\text{RSSe}^-/\text{RSSe}_2^-$  and  $\text{RSSe}_2^-/\text{RSSe}_3^-$  mixtures were assumed to give  $1 < \bar{y} < 2$  and  $2 < \bar{y} < 3$  respectively, with definite compositions linked to  $\bar{y}$  values (e.g.  $\bar{y} = 1.6$ , 40%  $\text{RSSe}^-$  and 60%  $\text{RSSe}_2^-$ ); (ii) for the most accurate conditions  $[\text{RS}_2\text{R}]_0 = [\text{Se}_x^{2-}]_0$ , the absorbances of  $\text{Se}_x^{2-}$  ions ( $x = 6, 8$  or  $4, 6$ ) calculated by the use of concentrations in Table 4 and characteristics in

Fig. 1 were subtracted from the experimental  $A$  values, 10 nm apart; (iii) the known spectra of  $\text{RSSe}^-$  ions ( $\text{RS}^- + 1 \text{Se}$ ,  $\epsilon_i \pm 5\%$ ) led firstly to those of  $\text{RSSe}_2^-$  ( $x = 4$ ), then  $\text{RSSe}_3^-$  ( $x = 6$ ). The  $A = f(\lambda)$  curves are reported in Fig. 8 for  $\text{R} = \text{Ph}$ , whereas Table 5 summarizes the spectrophotometric characteristics of  $\text{RSSe}_y^-$  ions ( $\text{R} = \text{Ph}, \text{PhCH}_2$ ;  $y = 1-3$ ).  $\lambda_{\text{max}}$  wavelengths of  $\text{RSSe}_y^-$  ions were lower by  $\approx 25$  nm than those of homologous  $\text{RSeSe}_y^-$  species ( $y = 1-3$ ), with close  $\epsilon_y$  values in both cases.<sup>1</sup> The formation of  $\text{RSSe}_4^-$  ions could not be proved from the addition of  $\text{RS}_2\text{R}$  disulfides to  $\text{Se}_8^{2-}$  ions, because of the detection of solid selenium within the solutions in the course of the reactions which entailed at first the shift  $A_{648} (\text{Se}_8^{2-}) \rightarrow A_{630} (\text{Se}_8^{2-}/\text{Se}_6^{2-})$ .

## Conclusions

Whereas selenolate ions undergo redox exchanges to  $\text{RSe}_2\text{R}$  diselenides with sulfur in *N,N*-dimethylacetamide, selenium adds to thiolates with the formation of the sulfur–selenium bond in  $\text{RSSe}^-$  species. The latter reactions, and those leading to  $\text{RSe}_2^-$  ( $\text{RSe}^- + \text{Se}$ ) which we recently reported, are analogous to the well known ‘S-nucleophilic processes’ affording  $\text{RS}_2^-$  ions from thiolates and sulfur.

In mixtures  $\text{RS}^- + \text{RSSe}^-$ ,  $\text{RSSe}^-$  ions oxidize into  $\text{RS}_2\text{R}$  faster than  $\text{RS}^-$  ions on a gold electrode, with a fast heterogeneous reaction between selenolate ions and electrogenerated selenium.  $\text{RSSeR}'$  alkylated selenenyl sulfides disproportionate to a large extent into symmetrical  $\text{RS}_2\text{R}$  and  $\text{R}'\text{Se}_2\text{R}'$  compounds.

$\text{RSSe}_y^-$  ions ( $y = 2, 3$ ), which partly disproportionate into  $\text{RS}_2\text{R}$  and  $\text{Se}_x^{2-}$  ions, result from the slow addition of solid Se to  $\text{RSSe}^-$  ions. The same equilibria are readily obtained by the reactions between  $\text{RS}_2\text{R}$  and  $\text{Se}_x^{2-}$  ions.

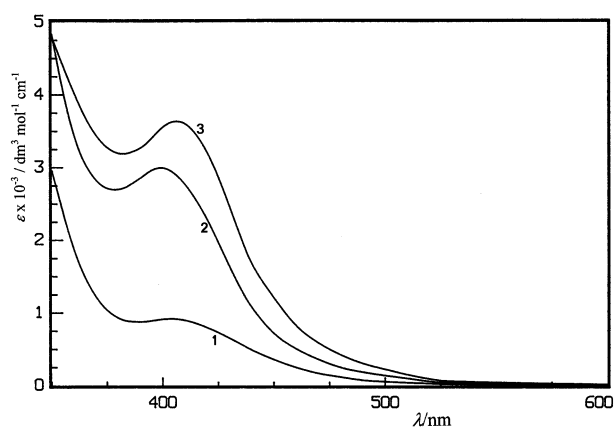


**Fig. 8** Calculated spectra ( $\epsilon_i/\text{dm}^3 \text{mol}^{-1} \text{cm}^{-1}$ ) of  $\text{PhSSe}_y^-$  ions.  $y = 1-3$ , (1)–(3).

**Table 5** Spectrophotometric characteristics of  $\text{RSSe}_y^-$  ions ( $y = 1\text{--}3$ ) in dimethylacetamide

R		$\text{RSSe}^-$	$\text{RSSe}_2^-$	$\text{RSSe}_3^-$
Ph	$\lambda_{\text{max}}^a/\text{nm}$	403	400	405
	$\epsilon_{\text{max}}^{b,c}$	900	3000	3600
$\text{PhCH}_2$	$\lambda_{\text{max}}^a/\text{nm}$	430	375	375
	$\epsilon_{\text{max}}^{b,c}$	400	2600	3000

<sup>a</sup>  $\lambda_{\text{max}}(y = 2, 3) \pm 4 \text{ nm}$ . <sup>b</sup>  $\epsilon_i/\text{dm}^3 \text{ mol}^{-1} \text{ cm}^{-1}$ . <sup>c</sup>  $\epsilon_i(y = 2, 3) \pm 15\%$ .

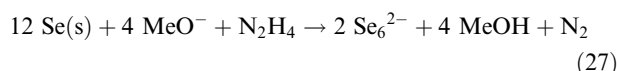
## Experimental

### Materials and equipment

*N,N*-Dimethylacetamide, grey selenium (99.999%, 100 mesh), and all the organic compounds were purchased from Aldrich except for diphenyl diselenide and dibenzyl mono- and diselenide (Acros Organics). Solvent purification and storage after addition of  $\text{NEt}_4\text{ClO}_4$  (Fluka,  $0.1 \text{ mol dm}^{-3}$ ) as supporting electrolyte have been reported elsewhere.<sup>17</sup> Spectroelectrochemical equipments and electrodes,<sup>1</sup> as well as the thermostatted ( $20.0 \pm 0.50^\circ\text{C}$ ) flow-through cell<sup>17</sup> have previously been described. All the potentials were referenced to  $\text{Ag}/\text{AgCl}$ ,  $\text{KCl}$  saturated in  $\text{DMA-NEt}_4\text{ClO}_4$  ( $0.1 \text{ mol dm}^{-3}$ ) electrode. The Se-coated gold foil was observed by Scanning Electron Microscopy (SEM FEG Gemini 982 Leo Microscope). The micrographs were obtained in secondary electron image mode (accelerating voltage of  $2 \text{ kV}$ ). The synthesized mixtures were analyzed by  $^1\text{H}$  NMR spectroscopy (200.132 MHz, Bruker AC 200) with  $\text{CDCl}_3$  as the solvent ( $\text{Me}_4\text{Si}$  as standard) and GC-MS (Hewlett-Packard 5989 A, EI  $70 \text{ eV}$ ).

### Generation of $\text{Se}_x^{2-}$ ions

Accurate concentrations of  $\text{Se}_x^{2-}$  ions were obtained by the same method as recently reported:<sup>1,2</sup> selenium was initially deposited on a large gold grid electrode [ $25 < w(\text{Se})/\text{mg} < 40$ ] by the electrooxidation ( $E = 0.0 \text{ V}$ ) of  $\text{Se}_x^{2-}$  solutions ( $\bar{x} \approx 6$ ) which were themselves chemically generated in DMA from the reduction of Se with hydrazine and sodium methoxide:<sup>18</sup>



The cathodic polarization of the Se-coated grid in DMA ( $40 \text{ cm}^3$ ) was then kept until the spectra and the related maximal absorbances of  $\text{Se}_x^{2-}$  (Fig. 1;  $x = 8$ ,  $E = -0.55 \text{ V}$ ;  $x = 6$ ,  $E = -0.75 \text{ V}$ ;  $x = 4$ ,  $E = -1.10 \text{ V}$ ) were attained. Concentrated solutions of  $\text{RS}_2\text{R}$  substrates in DMA ( $\text{R} = \text{Ph}$ ,  $\text{PhCH}_2$ ;  $v_{\text{max}} = 4 \text{ cm}^3$ ) were progressively added to  $\text{Se}_x^{2-}$  ions. In all cases, absorbances reached equilibrium within 1 min.

### Syntheses of $\text{RSSeR}'$ compounds

The  $\text{CH}_3\text{SSe}^- + \text{PhCH}_2\text{Br}$  and  $\text{PhSSe}^- + \text{CH}_3\text{I}$  reactions were carried out according to the same procedure on a preparative scale: solid sodium thiomethoxide (95%) and lithium thiophenoxide ( $1 \text{ mol dm}^{-3}$  in THF) of commercial origin were dissolved in  $80 \text{ cm}^3$  of deaerated DMA under an  $\text{N}_2$  atmosphere. The  $\text{RS}^-$  solutions were stirred at  $50^\circ\text{C}$  with selenium powder ( $\text{Se}:\text{RS}^- = 1:1$ ) which reacted within 3 hours. Stoichiometric amounts of alkyl halides dissolved in DMA ( $20 \text{ cm}^3$ ) were then added dropwise (20 min) at room temperature to the yellow  $\text{RSSe}^-$  solutions. After filtration ( $0^\circ\text{C}$ ) of the medium and addition of water ( $300 \text{ cm}^3$ ), the products were extracted with diethyl ether. The organic phase was thoroughly washed with water (elimination of residual DMA) and dried over  $\text{MgSO}_4$ . After evaporation *in vacuo*, the mixtures

were rapidly analyzed without attempting to separate the individual compounds because of the poor stability of the  $\text{RSSeR}'$  species.<sup>10,11</sup>

**Reaction of  $\text{CH}_3\text{SSe}^-$  ions with  $\text{PhCH}_2\text{Br}$ .**  $\text{CH}_3\text{S}^-\text{Na}^+$  ( $0.814 \text{ g}$ ,  $11.6 \text{ mmol}$ ), Se ( $0.909 \text{ g}$ ,  $11.5 \text{ mmol}$ ),  $\text{PhCH}_2\text{Br}$  ( $1.40 \text{ cm}^3$ ,  $11.5 \text{ mmol}$ ). The composition of the mixture of products ( $1.97 \text{ g}$ ):  $\text{CH}_3\text{SSeCH}_2\text{Ph}$  (29%),  $(\text{PhCH}_2)_2\text{Se}_2$  (57%),  $(\text{CH}_3\text{S})_2$  (14%), was determined from  $\delta_{\text{H}}$  (s, 2H) and  $\delta_{\text{H}}$  (s, 3H);  $(\text{CH}_3\text{S})_2$  and  $(\text{PhCH}_2)_2\text{Se}_2$  were identified by the use of commercial samples which were added to the synthesized mixture. Volatile  $(\text{CH}_3\text{S})_2$  was assumed to have been greatly reduced in the course of the solvent evaporation. The disproportionation level of  $\text{CH}_3\text{SSeCH}_2\text{Ph}$  ( $\approx 80\%$ ) was thus calculated by reference to the only  $(\text{PhCH}_2)_2\text{Se}_2$  proportion.  $(\text{PhCH}_2)_2\text{Se}_2$ , which gave no  $^1\text{H}$  NMR signal, was detected in the mass spectra as a result of the known selenium extrusion from benzylic diselenide under thermal conditions.<sup>19</sup>  $\text{CH}_3\text{SSeCH}_2\text{Ph}$ :  $\delta_{\text{H}}$  2.24<sub>s</sub> (s, 3H), 4.08 (s, 2H);  $m/z$  218 ( $^{80}\text{Se}$ ,  $\text{M}^+$ , 4%), 91 (100), 65(16) and 39 (9).  $(\text{PhCH}_2)_2\text{Se}_2$ :  $\delta_{\text{H}}$  3.80 (s, 4H);  $m/z$  342 ( $^{80}\text{Se}$ ,  $\text{M}^+$ , 2%), 91 (100).  $(\text{CH}_3\text{S})_2$ :  $\delta_{\text{H}}$  2.39<sub>s</sub> (6H, s;  $m/z$  96 ( $\text{M}^+ + 2$ , 11), 94 ( $\text{M}^+$ , 100%).  $(\text{PhCH}_2)_2\text{Se}$ :  $m/z$  262 ( $^{80}\text{Se}$ ,  $\text{M}^+$ , 7%), 91 (100).

**Reaction of  $\text{PhSSe}^-$  with  $\text{CH}_3\text{I}$ .**  $\text{PhS}^-\text{Li}^+$  in THF ( $11 \text{ cm}^3$ ,  $11 \text{ mmol}$ ), Se ( $0.792 \text{ g}$ ,  $10.0 \text{ mmol}$ ),  $\text{CH}_3\text{I}$  ( $0.80 \text{ cm}^3$ ,  $12.8 \text{ mmol}$ ). The products were identified both by  $^1\text{H}$  NMR with the use of commercial samples of  $(\text{PhS})_2$ ,  $(\text{CH}_3\text{Se})_2$  and  $\text{PhSCH}_3$  compounds, and by GC-MS. The composition of the mixture ( $1.79 \text{ g}$ ):  $\text{PhSSeCH}_3$  (32%),  $(\text{PhS})_2$  (35%),  $(\text{CH}_3\text{Se})_2$  (22%) and  $\text{PhSCH}_3$  (11%, close to the initial ratio  $\text{PhS}^-:\text{PhSSe}^- = 1:10$ ), was determined by combining the integrals of  $\delta_{\text{H}}$  (s, 3H) with those of aromatic  $\delta_{\text{H}}$ ,  $(\text{PhS})_2$  (4 Ho) and  $\text{PhSSeCH}_3$  (2Ho). It was in good agreement with the integration of the GC peaks. Here again, the disproportionation of  $\text{PhSSeCH}_3$  ( $\approx 70\%$ ) was evaluated from the respective proportions of  $\text{PhSSeCH}_3$  and  $(\text{PhS})_2$  in the mixture.  $\text{PhSSeCH}_3$ :  $\delta_{\text{H}}$  2.46 (s, 3H), 7.51 (1Ho, Ar), 7.55 (1Ho, Ar);  $m/z$  204 ( $^{80}\text{Se}$ ,  $\text{M}^+$ , 87%), 189 (57), 109 (100), 77 (51), 69 (37), 65 (76), 51 (43), 39 (49).  $(\text{PhS})_2$ :  $\delta_{\text{H}}$  7.45 (2Ho, Ar), 7.49 (2Ho, Ar);  $m/z$  218 ( $\text{M}^+$ , 76%).  $(\text{CH}_3\text{Se})_2$ :  $\delta_{\text{H}}$  2.67<sub>s</sub> (s, 6H);  $m/z$  190 ( $^{80}\text{Se}$ ,  $\text{M}^+$ , 88%).  $\text{PhSCH}_3$ :  $\delta_{\text{H}}$  2.44<sub>s</sub> (s, 3H);  $m/z$  124 ( $\text{M}^+$ , 100%).

## References

- 1 A. Ahrika, J. Robert, M. Anouti and J. Paris, *New J. Chem.*, 2001, **25**, 741.
- 2 A. Ahrika and J. Paris, *New J. Chem.*, 1999, **23**, 1177.
- 3 G. Bosser, M. Anouti and J. Paris, *J. Chem. Soc., Perkin Trans. 2*, 1996, 1993.
- 4 C. Kölleman, D. Obendorf and F. Sladsky, *Phosphorus Sulfur Relat. Elem.*, 1988, **38**, 69.
- 5 A. Ahrika, J. Auger and J. Paris, *New J. Chem.*, 1999, **23**, 679.
- 6 M. Benaïchouche, G. Bosser, J. Paris, J. Auger and V. Plichon, *J. Chem. Soc., Perkin Trans. 2*, 1990, 31.
- 7 E. Block, in *Dietary Phytochemicals in Cancer Prevention and Treatment*, Plenum Press, New York, 1996, pp. 155–169 and references cited therein.
- 8 C. Ip and D. J. Lisk, in *Dietary Phytochemicals in Cancer Prevention and Treatment*, Plenum Press, New York, 1996, pp. 179–187.
- 9 X.-J. Cai, P. C. Uden, E. Block, X. Zhang, B. D. Quimby and J. J. Sullivan, *J. Agric. Food Chem.*, 1994, **42**, 2081.
- 10 (a) H. Rheinbolt and E. Giesbrecht, *Liebigs Ann. Chem.*, 1950, 198; (b) H. H. Sisler and N. K. Kotia, *J. Org. Chem.*, 1971, **36**, 1700; (c) J. L. Kice and T. W. S. Lee, *J. Am. Chem. Soc.*, 1978, **100**, 5094; (d) M. Yoshida, T. Cho and M. Kobayashi, *Chem. Lett.*, 1984, 1109.
- 11 (a) W. Mc Farlane, *J. Chem. Soc. (A)*, 1969, 913; (b) V. A. Potapov, S. V. Amosova, P. A. Petrov, L. S. Romanenko and V. V. Keiko, *Sulfur Lett.*, 1992, **15**, 121.
- 12 F. Gaillard and E. Levillain, *J. Electroanal. Chem.*, 1995, **398**, 77 and references cited therein.

- 13 G. Bosser and J. Paris, *New J. Chem.*, 1995, **19**, 391.  
14 K. W. Sharp and W. H. Koelher, *Inorg. Chem.*, 1977, **16**, 2258.  
15 (a) C. Degrand, *J. Chem. Soc., Chem. Commun.*, 1986, 1113;  
(b) C. Degrand and R. Prest, *J. Org. Chem.*, 1990, **55**, 5242.  
16 (a) F. Magno, G. Bontempelli and G. Pilloni, *J. Electroanal. Chem.*, 1971, **30**, 375; (b) M. Liu, S.-J. Visco and L. C. De Jonghe, *J. Electrochem. Soc.*, 1989, **136**, 2570.  
17 J. Paris and V. Plichon, *Electrochim. Acta*, 1981, **26**, 1823.  
18 H. Eggert, O. Nielsen and L. Henriksen, *J. Am. Chem. Soc.*, 1986, **108**, 1725.  
19 (a) M. A. Lardon, *Ann. N.Y. Acad. Sci.*, 1972, **192**, 132; (b) J. Y. Chu and J. W. Lewicki, *J. Org. Chem.*, 1977, **42**, 2491.